Int. J. Multiphase Flow Vol. 15, No. 5, pp. 803–814, 1989
Printed in Great Britain.

0301-9322/89 $3.00 + 0.00

ENHANCEMENT OF HEAT TRANSFER DUE TO BUBBLES PASSING THROUGH A NARROW VERTICAL RECTANGULAR CHANNEL

M. MONDE and Y. MITSUTAKE
Department of Mechanical Engineering, Saga University, 1 Honjo Saga, 840 Japan

(*Received* 1 *February* 1989; *in revised form* 12 *June* 1989)

Abstract—A theoretical analysis has been made of heat transfer enhancement due to bubbles passing through a narrow vertical channel. The mechanism of enhancement for a constant heat flux is: heat is first transported by a latent heat of evaporation on the bubble interface covering the heated surface and is followed by sensible heating of the succeeding liquid. The latent heat transport is calculated using an integral method and the sensible heating is determined exactly. For low heat fluxes, the calculated heat transfer coefficients are in fairly good agreement with the experiments; at high heat fluxes, however, the calculated values are approximately half the experimental values, since flow along the heated surface is not taken into account.

Key Words: phase change, heat transfer, enhancement, confined space, vertical rectangular channel, passing bubble

1. INTRODUCTION

Heat transfer is markedly enhanced when bubbles generated on a heated surface in a narrow space pass through the gap under conditions of bubble or slug flow (Ishibashi & Nishikawa 1960; Nakashima 1978; Kusuda *et al.* 1981; Monde *et al.* 1986, 1988; Monde 1988, 1989). The mechanism of the enhancement can be explained from two different points of view: first, the transient thermal conduction model by Ishibashi & Nishikawa (1960) in which 70% of the total heat transfer is transported by convection and the remainder by latent heat; and second, the evaporation model by Nakashima (1978) that states that the thermal transport is mainly by evaporation of the liquid film which appears when a bubble passes by the surface.

In the first model it is assumed that the surface temperature remains constant in spite of the temperature fluctuations caused by passing bubbles. In addition, the analysis differs from reality because evaporation of the surface liquid film depends on the heat flux and bubble frequency. These effects should cause differences between theoretical and experimental results. On the other hand, the second model derives a correlation predicting the heat transfer coefficient, $\bar{h}$, for a mean duration time of $t_b = 0.0205$ s, during which the passing bubbles cover a heated tube, based on the assumption that the liquid film is between 28–47 μm thick.

Kusuda *et al.* (1981) measured the temperature change of the heated surface due to the passing bubbles by using an electrically heated stainless steel foil as the heated surface. They proposed an enhancement model based on the relationship between the change in the surface temperature and the period of the passing bubbles. Although comparison of the theoretical and experimental results was made based on the assumption that the thickness of liquid film was 50 μm, the mechanism of enhancement could not be discerned.

Recently, Monde (1989) has measured the thickness of the liquid film when a bubble passes through a narrow vertical rectangular channel. Monde *et al.* (1989) have also clearly determined the basis of the enhancement in a subcooled liquid, and thus, without evaporation, based upon a theoretical result proposed by Monde (1988).

The present study will account for both the effects of evaporation and convection on the basis of the change in the heated surface temperature during one cycle of the passing bubble. The theoretical results will be compared with the experiments.

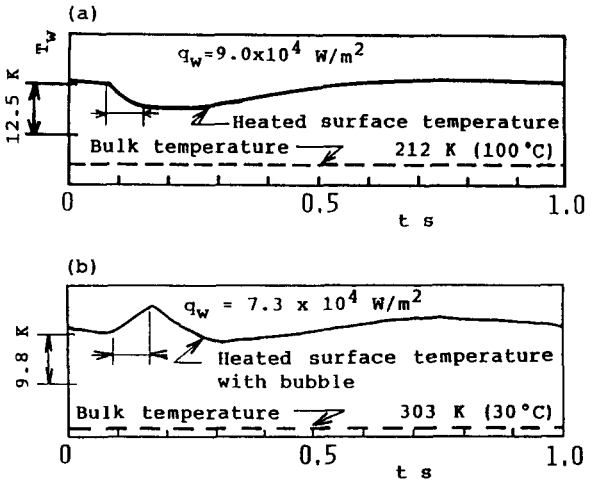

Figure 1. Temperature change of the heated surface due to the passing of a bubble during one cycle: (a) $\Delta T_{sub} = 0$ K; (b) $\Delta T_{sub} = 70$ K.

2. THEORETICAL ANALYSIS AND ITS SOLUTION

The model of Kusuda *et al.* (1981) for heat transfer enhancement, will first be briefly explained. This model is based on the assumptions that: (i) most of the superheated liquid is swept away by the bubble passing along the heated surface; (ii) a stationary thin liquid film always remains between the heated surface and the passing bubble, however evaporation from its surface can be ignored; and (iii) the stationary liquid at the bulk temperature immediately covers the heated surface after the bubble passes. Based on these assumptions, the problem can be treated as heat conduction in a semi-infinite solid, since the thickness of the remaining liquid film is very thin compared with the width of the narrow space; namely, the ratio of its thickness to its width is less than one-tenth and the value of $\sqrt{at_0}$ is on the order of 10^{-4} m, where a is thermal diffusivity and T_0 is the period of the passing bubble. In a recent study by Monde (1988), using the Kusuda *et al.* model, the characteristics of the solutions for two special cases of heated surfaces with a constant heat flux and a constant temperature are developed, including the two limiting states of δ ($= S_0/\sqrt{aT_0}$; S_0—initial thickness of the liquid film) $= 0$ and ∞.

The recent experiments by Monde *et al.* (1986, 1989), show that the temperature changes in the heated surface during one cycle, differ significantly for the saturated and subcooled liquid cases [figures 1(a,b)]. In the saturated liquid the temperature suddenly drops immediately the bubble reaches the heated surface, while in the subcooled liquid the temperature rises. This difference in behavior results from the evaporation of the liquid film on the interface when the bubble covers the heated surface. The present study, therefore corrects the Kusuda *et al.* (1981) model by attempting to account for the evaporation as follows: the heated surface is first cooled by evaporation for the time duration from $t = 0$ to t_b during which it is covered by the passing bubble; liquid from the saturation liquid flows into the space immediately after the bubble passes, as shown in figure 2. Flow along the heated surface is ignored, as in Kusuda *et al.* (1981). The resulting analysis is made up of two parts: (I) latent heat transport by evaporation; and (II) sensible heat transport by liquid.

(I) Latent heat transport by evaporation ($0 < t < t_b$)

The basic equation in the liquid film during $0 < t < t_b$ is

$$\rho c \frac{\partial T}{\partial t} = \lambda \frac{\partial^2 T}{\partial x^2}, \qquad [1]$$

with the boundary conditions

$$-\lambda \frac{\partial T}{\partial x} = q_w. \qquad x = 0, \quad t > 0, \qquad [2]$$

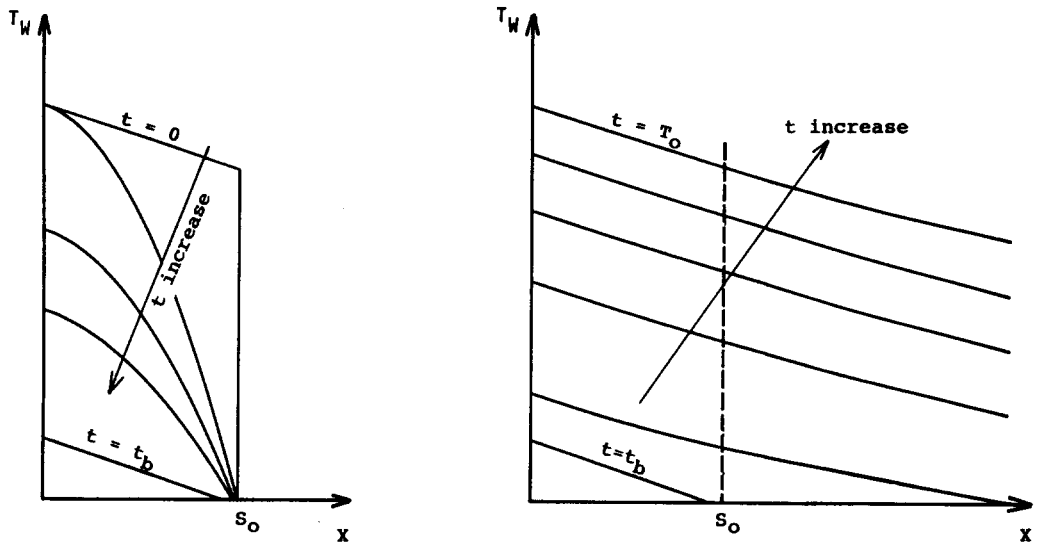

Figure 2. Physical model for enhancement.

$$T = T_{sat}, \qquad x = S(t), \quad t > 0, \tag{3}$$

and

$$\lambda \frac{\partial T}{\partial x} = \rho h_{LG} \frac{dS}{dt}, \qquad x = S(t), \quad t > 0; \tag{4}$$

where ρ is the liquid density, c is the specific heat of liquid, λ is the thermal conductivity, h_{LG} is the latent heat of evaporation, T is temperature of the liquid film, T_{sat} is the saturation temperature, q_w is the heat flux at the heated surface, $S(t)$ is the thickness of liquid film and x is distance from the heated surface. Equation [4] represents the energy balance on the interface. The resulting non-linear equation makes an exact solution difficult and requires an approximate method of solution. An integral approximation of [1] together with [2]–[4], results in

$$\frac{d}{dt}\int_0^{S(t)} \rho c(T - T_{sat})\, dx = q_w + \rho h_{LG} \frac{dS}{dt}. \tag{5}$$

An approximate temperature distribution in the liquid film based upon a second-degree polynomial in x, and assumed with coefficients which satisfy [2] and [3], yields

$$T(x,t) - T_{sat} = -\frac{\rho h_{LG}\left(\frac{dS}{dt}\right) + q_w}{2\lambda S}(S^2 - x^2) + \frac{q_w}{\lambda}(S - x). \tag{6}$$

By substitution of [6] into [5] and rearranging, a non-linear ordinary differential equation in terms of the thickness of the liquid film results, i.e.

$$\frac{d^2S}{dt^2} + \frac{2\left(\frac{dS}{dt}\right)^2}{S} + \left(3a - \frac{q_w S}{\rho h_{LG}}\right)\frac{\left(\frac{dS}{dt}\right)}{S^2} + 3\frac{aq_w}{\rho h_{LG} S^2} = 0, \tag{7}$$

with the initial conditions

$$S(0) = S_0 \tag{8}$$

and

$$\frac{dS(0)}{dt} = \frac{q_w}{\rho h_{LG}} - 2\frac{\lambda}{\rho h_{LG} S_0}(T_{w0} - T_{sat}). \tag{9}$$

This may be made non-dimensional by substituting the parameters (ξ_1, τ, δ_1, α, θ):

$$\theta(\xi_1,\tau) = -\frac{S_0}{2\lambda(T_{w0}-T_{sat})\delta_1}\left[\frac{\rho h_{LG} S_0\left(\frac{d\delta_1}{d\tau}\right)}{T_0} + q_w\right](\delta_1^2-\xi_1^2) + \frac{q_w S_0}{\lambda(T_{w0}-T_{sat})}(\delta_1-\xi_1), \quad [10]$$

$$\frac{d^2\delta_1}{d\tau^2} + \frac{2}{\delta_1}\left(\frac{d\delta_1}{d\tau}\right)^2 + (3A_1 - A_2\delta_1)\frac{\left(\frac{d\delta_1}{d\tau}\right)}{\delta_1^2} + \frac{3A_1A_2}{\delta_1^2} = 0, \quad [11]$$

$$\delta_1(0) = 1 \quad [12]$$

and

$$\frac{d\delta_1(0)}{d\tau} = A_2 - A_3, \quad [13]$$

where

$$A_1 = \frac{aT_0}{S_0^2}, \qquad A_2 = \frac{q_w T_0}{(\rho h_{LG} S_0)},$$

$$A_3 = \frac{2\lambda(T_{w0}-T_{sat})T_0}{(\rho h_{LG} S_0^2)}, \qquad \theta = \frac{(T-T_{sat})}{(T_{w0}-T_{sat})},$$

$$\xi_1 = \frac{x}{S_0}, \qquad \tau = \frac{t}{T_0},$$

$$\delta_1 = \frac{S(t)}{S_0}.$$

The solution for δ_1, $0 < \tau < \alpha\ (= t_b/T_0)$ can be determined using the Runge–Kutta–Gill procedure. The temperature distribution and the heated surface temperature can then be calculated as

$$\theta_w(0,\tau) = -\frac{S_0}{2\lambda(T_{w0}-T_{sat})}\left[\frac{\rho h_{LG} S_0\left(\frac{d\delta_1}{d\tau}\right)}{T_0} - q_w\right]\delta_1. \quad [14]$$

The temperature distribution at $\tau = \alpha$, when the bubble passes the heated surface, becomes

$$\theta(\xi_1,\alpha) = -\frac{S_0}{2\lambda(T_{w0}-T_{sat})\delta_b}\left[\frac{\rho h_{LG} S_0\left(\frac{d\delta_b}{d\tau}\right)}{T_0} + q_w\right](\delta_b^2-\xi_1^2) + \frac{q_w S_0}{\lambda(T_{w0}-T_{sat})}(\delta_b-\xi_1), \quad [15]$$

where δ_b is the non-dimensional film thickness at $\tau = \alpha$.

(II) Sensible heat transport by liquid ($t_b < t < T_0$)

In the liquid, heat conduction for the time interval of $t_b < t < T_0$ becomes, for $0 < x$:

$$\rho c\frac{\partial T}{\partial t} = \lambda\frac{\partial^2 T}{\partial x^2}, \quad [16]$$

with the boundary conditions

$$-\lambda\frac{\partial T}{\partial x} = q_w, \qquad x = 0, \quad [17a]$$

$$T = T_{sat}, \qquad x \to \infty, \quad [17b]$$

and the initial conditions at $t = t_b$,

$$T(x, t) - T_{sat} = \theta(\xi_1, \alpha)(T_{w0} - T_{sat}), \qquad 0 < x < S_2, \tag{18a}$$

$$T(x, t) = T_{sat}, \qquad S_2 < x, \tag{18b}$$

where S_2 is thickness of the liquid film at $t = t_b$.

Non-dimensional equations result by substituting the non-dimensional parameters (ξ_2, τ, δ_2) into [16]–[18], i.e.

$$\frac{\partial\theta}{\partial\tau} = \frac{\partial^2\theta}{\partial\xi_2^2}, \qquad 0 < \xi_2, \quad \alpha < \tau < 1, \tag{19}$$

$$\frac{\partial\theta}{\partial\xi_2} = \begin{cases} -B_1, & \xi_2 = 0 \\ 0, & \xi_2 \to \infty \end{cases} \tag{20}$$

and

$$\theta(\xi_2, \alpha) = \begin{cases} \theta(\xi_1, \alpha) = f(\xi_2), & 0 < \xi_2 < \delta_2 \\ 0, & \delta_2 < \xi_2, \end{cases} \tag{21}$$

where $f(\xi_2)$ in [21] can be obtained by rearranging [15] in the form

$$f(\xi_2) = -B_2\xi_2^2 - B_1\xi_2 + (B_2\delta_2^2 + B_1\delta_2), \tag{22}$$

and

$$B_1 = \frac{q_w\sqrt{aT_0}}{[\lambda(T_{w0} - T_{sat})]},$$

$$B_2 = -\frac{a}{2\lambda(T_{w0} - T_{sat})\delta_b}\left[\rho h_{LG}\left(\frac{d\delta_b}{d\tau}\right) + \frac{q_w T_0}{S_0}\right],$$

$$\xi_2 = \frac{x}{\sqrt{aT_0}}$$

and

$$\delta_2 = \frac{S_2}{\sqrt{aT_0}}.$$

The solution of [19] that satisfies [20] and [21] is given by [23]. The resulting temperature of the heated surface is given by [24]:

$$\begin{aligned}\theta(\xi_2, \tau_2) = {} & (B_2\delta_2 + 0.5B_1)\left(2\sqrt{\frac{\tau_2}{\pi}}\left\{\exp\left[-\frac{(\delta_2 + \xi_2)^2}{4\tau_2}\right] + \exp\left[-\frac{(\delta_2 - \xi_2)^2}{4\tau_2}\right]\right\}\right. \\ & \left. - \left[(\delta_2 + \xi_2)\operatorname{erfc}\left(\frac{\delta_2 + \xi_2}{2\sqrt{\tau_2}}\right) + (\delta_2 - \xi_2)\operatorname{erfc}\left(\frac{\delta_2 + \xi_2}{2\sqrt{\tau_2}}\right)\right]\right) \\ & + B_2\left(\left[\tau_2 + \frac{(\delta_2 + \xi_2)^2}{2}\right]\operatorname{erfc}\left(\frac{\delta_2 + \xi_2}{2\sqrt{\tau_2}}\right) + \left[\tau_2 + \frac{(\delta_2 - \xi_2)^2}{2}\right]\operatorname{erfc}\left(\frac{\delta_2 - \xi_2}{2\sqrt{\tau_2}}\right)\right. \\ & \left. - \sqrt{\frac{\tau_2}{\pi}}\left\{(\delta_2 + \xi_2)\exp\left[-\frac{(\delta_2 + \xi_2)^2}{4\tau_2}\right]\right.\right. \\ & \left.\left. + (\delta_2 - \xi_2)\exp\left[-\frac{(\delta_2 - \xi_2)^2}{4\tau_2}\right]\right\}\right) + f(\xi_2) - 2B_2\tau_2\end{aligned} \tag{23}$$

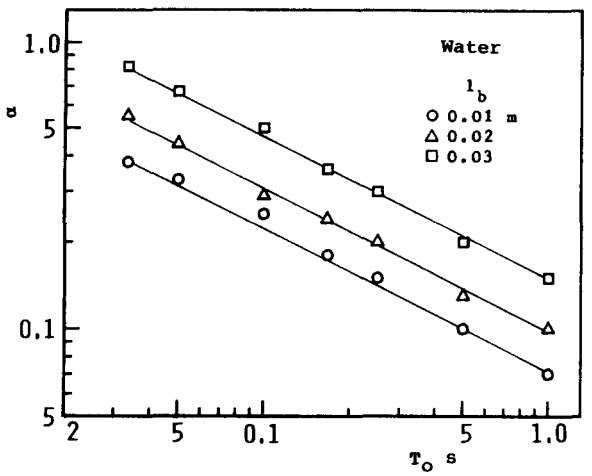

Figure 3. Relationship between the non-dimensional residence time and the period of the passing bubble.

and

$$\theta_w(\tau_2) = (B_2\delta_2 + B_1)\left\{2\sqrt{\frac{\tau_2}{\pi}}\exp\left[-\frac{(\delta_2)^2}{4\tau_2}\right] + \delta_2\,\mathrm{erf}\left(\frac{\delta_2}{2\sqrt{\tau_2}}\right)\right\} - 2B_2\tau_2\,\mathrm{erf}\left(\frac{\delta_2}{2\sqrt{\tau_2}}\right), \qquad [24]$$

where τ_2 in [23] and [24] is $\tau_2 = \tau - \alpha$.

In order to complete the calculations, it is necessary to know the initial thickness of the liquid film, S_0, the non-dimensional residence time of the bubble, α, and the initial temperature of the heated surface, T_{w0}.

The initial thickness and the non-dimensional residence time can be determined from analysis of the flow pattern of the bubble passing through the channel. According to the work of Monde (1989), the thickness of the liquid film while the bubble passes through the channel, $S_0 = 71.7\,\mu$m, is independent of the bubble period T_0 (= 0.1–1.0 s) and bubble length l_b (= 0.01–0.03 m). A value of $S_0 = 71.7\,\mu$m is therefore adopted.

The non-dimensional residence time can be determined from the velocity and bubble length of the rising bubble, as in the experiments (Monde *et al.* 1988).

Figure 3 shows the values of α plotted against period for $T_0 = 0.033$–1.0 s. The relation between α and T_0 may be obtained in this region as

$$\alpha = CT_0^{-0.5}, \qquad [25]$$

where

$$\begin{array}{lll} C = 0.15 & \text{for} & l_b = 0.03\ \text{m} \\ 0.10 & & 0.02 \\ 0.071 & & 0.01. \end{array}$$

The initial temperature, T_{w0}, is however still unknown, but can be determined from the periodic condition in an iterative fashion: first the numerical calculation is performed by providing an estimated initial value for T_{w0}, yielding [15] and a temperature at $t = T_0$, namely $\tau_2 = 1 - \alpha$ can be calculated from [24]. This procedure is continued until the difference between the calculated and the assumed values becomes $< 10^{-3}$.

3. THEORETICAL RESULT

3.1. Change of liquid film thickness during evaporation

Figure 4 shows the relationship between the non-dimensional liquid film thickness and the time period of evaporation. It is seen that the thickness decreases sharply during the time period $\tau = 0$

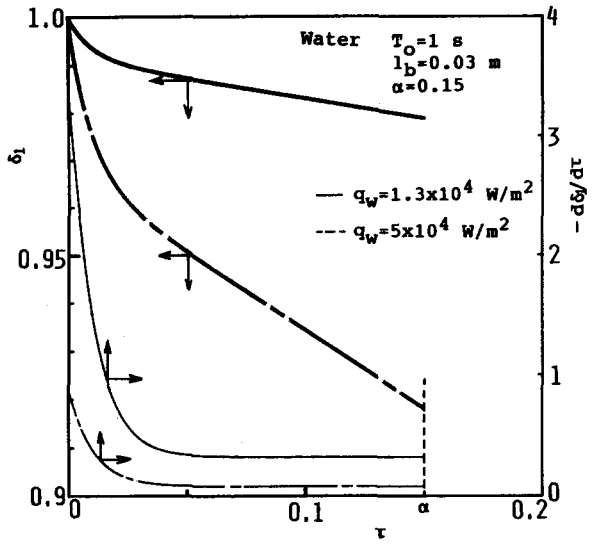

Figure 4. Variation of film thickness during interface evaporation.

to about 0.25α. It then gradually decreases, corresponding to the situation that the heat transferred from the heated surface to the interface is consumed by the evaporation at the interface. This condition also means that the temperature distribution in the liquid film is linear.

3.2. Temperature change of the heated surface during one cycle

Figure 5(a) shows a typical temperature change of the heated surface caused by the passing of a bubble ($l_b = 0.02$ m) at a heat flux of $q_w = 1.3 \times 10^4$ W/m^2 during one cycle. Figure 5(b) shows the typical temperature change for the period $T_0 = 0.25$ s also at $q_w = 1.3 \times 10^4$ W/m^2. The non-dimensional residence time in figure 5 can be calculated from [25].

It is seen from figures 5(a, b) that the temperature of the heated surface sharply drops during the time of $\tau = 0$ to $\tau = 0.25\alpha$ and then gradually decreases until $\tau = \alpha$. The temperature change corresponds to the decrease in the liquid film thickness since the heat transferred from the heated

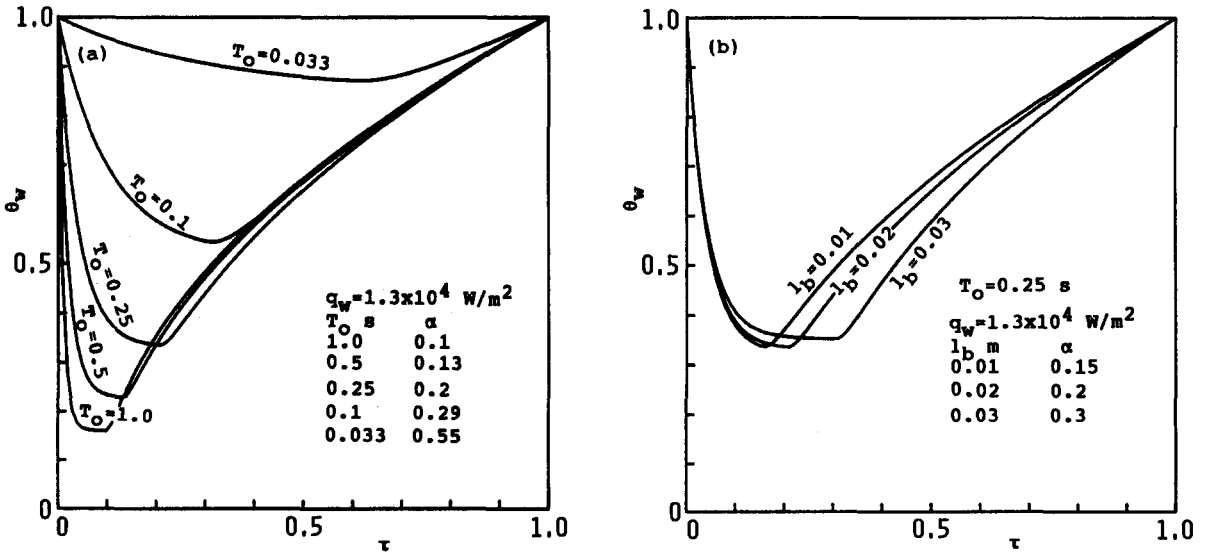

Figure 5. Temperature change of the heated surface during one cycle (theoretical result): (a) effect of period; (b) effect of bubble length.

surface is controlled by the evaporation of the liquid film on the interface. After the bubble passes, namely $\tau > \alpha$, the temperature gradually recovers. In figure 5(a), the temperature change is not critically dependent on the period, bringing about the increase in α and at last disappears below a certain period. From figure 5(b), the temperature recovery is delayed as α increases with the increase in the bubble length.

3.3. *Time-averaged heat transfer coefficient*

A time-averaged heat transfer coefficient can be defined as

$$\bar{h} = \frac{1}{T_0}\int_0^{T_0} \frac{q_w}{T_w(t) - T_{sat}}\,dt. \qquad [26]$$

The non-dimensional heat transfer coefficient $\bar{h}\sqrt{aT_0}/\lambda$ can be introduced to give

$$\frac{\bar{h}\sqrt{aT_0}}{\lambda} = B_1\left[\int_0^{\alpha} \theta_w^{-1}(\tau)\,d\tau + \int_0^{1-\alpha} \theta_w^{-1}(\tau_2)\,d\tau_2\right]. \qquad [27]$$

The non-dimensional temperatures $\theta_w(\tau)$ and $\theta_w(\tau_2)$ are given by [14] and [24], respectively so that the value of $\bar{h}\sqrt{aT_0}/\lambda$ can be calculated numerically.

Figure 6 indicates the heat transfer calculated from [27] as a function of δ; $\delta = S_0/\sqrt{aT_0}$. The scale of T_0 is chosen as the value of T_0 for water, calculated from $\delta = S_0/\sqrt{aT_0}$ using $S_0 = 71.7\ \mu$m. The thin solid line represents the limiting solution without evaporation ($\alpha = 0$), while the dashed line is the limiting solution ($\alpha = 1$) under which the temperature change of the heated surface does not occur and the flow pattern becomes one of annular flow. In addition, this situation will appear for $\delta > 3$. In the region above the ——— line in figure 6, experimental results are difficult to obtain.

Figure 7 shows the relationship between $\bar{h}\sqrt{aT_0}/\lambda$ and α. It is seen that evaporation has a significant effect on the heat transfer as the residence time α becomes small. The heat transfer becomes independent of α at $\delta = 0.8$ due to the fact that the enhancement of the heat transfer has reached an upper limit.

Figure 8 illustrates the ratio of evaporation heat transport to the total amount of heat transport during one cycle plotted against non-dimensional residence time, α. It can be seen that the amount

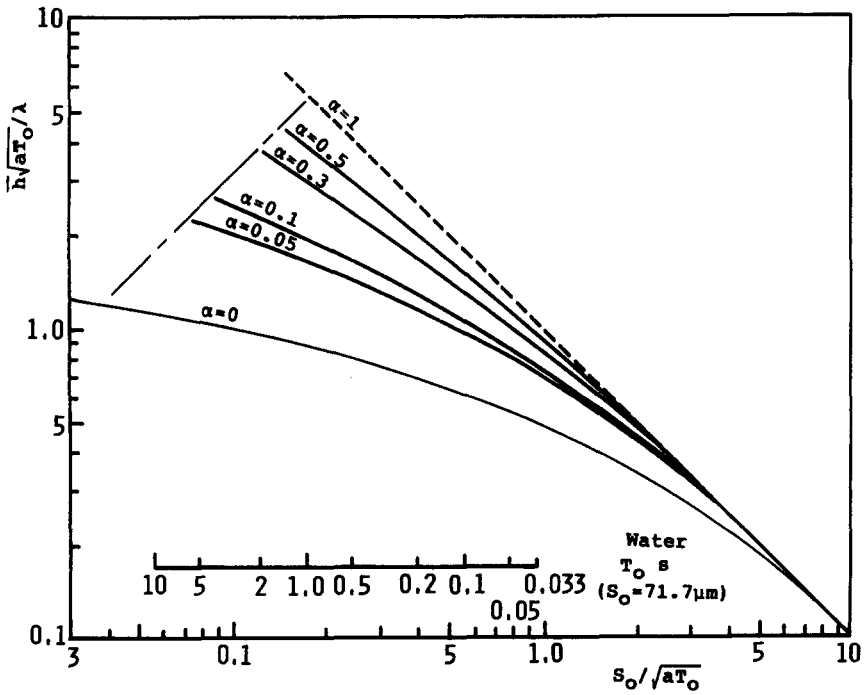

Figure 6. Dimensionless heat transfer, $\bar{h}\sqrt{aT_0}/\lambda$, as a function of dimensionless film thickness, $\delta = S_0/\sqrt{aT_0}$ (theoretical result).

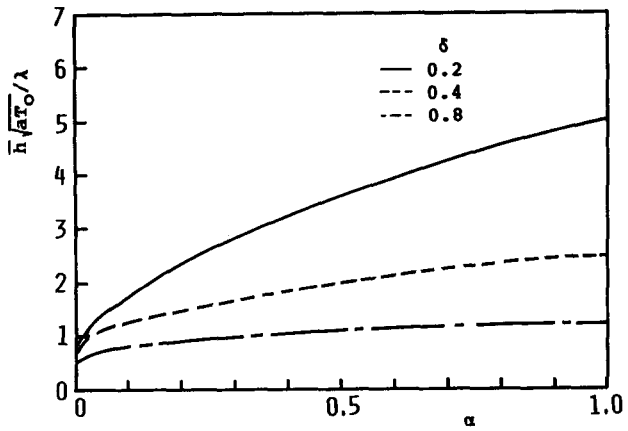

Figure 7. Dimensionless heat transfer, $\bar{h}\sqrt{aT_0}/\lambda$, as a function of dimensionless residence time, α.

of the heat transported by the evaporation increases with the increase in α and more than half of the total amount is transported for $\alpha > 0.32$ by evaporation.

4. COMPARISON OF THE THEORETICAL AND EXPERIMENTAL RESULTS

4.1. Temperature change of the heated surface during one cycle

Figures 9(a, b) represents a typical temperature change during one cycle. The thick solid lines in figures 9(a, b) are the experimental results of Monde *et al.* (1986, 1988) and the thin solid lines are the calculated ones. Figure 9(a) shows that both results are in a good agreement for low heat flux ($q_w = 1.3 \times 10^4$ W/m^2); there are however differences for high heat flux ($q_w = 9.0 \times 10^4$ W/m^2) [figure 9(b)]. The difference can be attributed to the effects of the flow along the heated surface which was not considered in the analysis. Flow effects become significant at high heat flux for two reasons: first, the heated surface temperature recovery becomes faster, so that the liquid temperature rise in a thermal boundary layer becomes faster; and second, the experiment is carried out under the condition that the liquid without the thermal boundary layer suddenly flows into the heated surface. If the heated surface is sufficiently long and a thermal boundary layer develops,

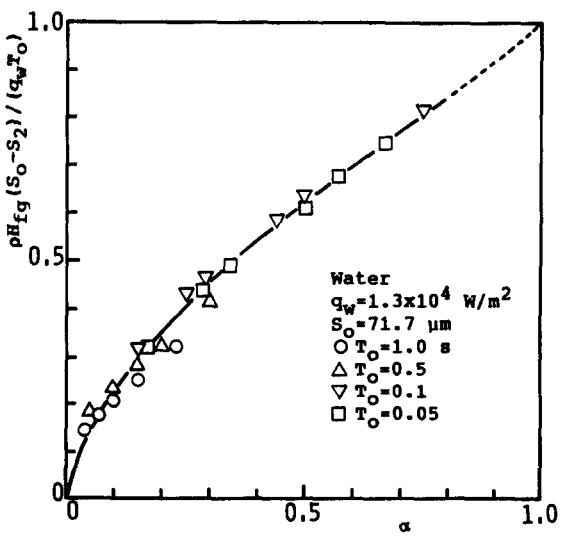

Figure 8. Amount of heat transported by evaporation vs dimensionless residence time, α.

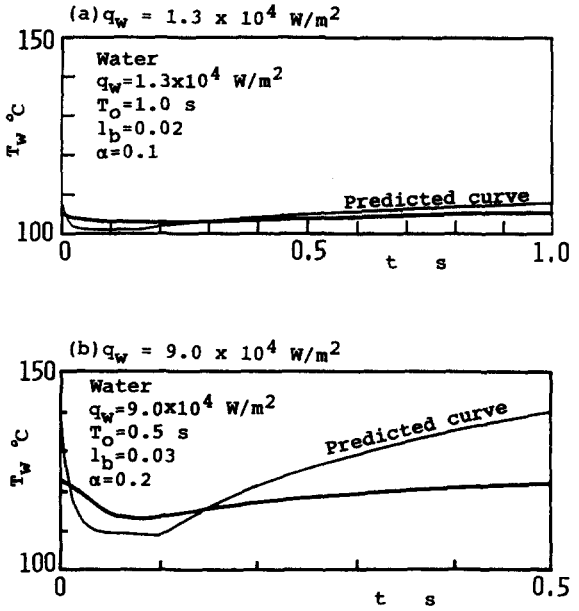

Figure 9. Comparison of temperature changes calculated and measured during one cycle at (a) a low heat flux of $q_w = 1.3 \times 10^4$ w/m^2 and (b) a high heat flux of $q_w = 9.0 \times 10^4$ w/m^2.

the flow effect becomes small compared with that on the short heated surface. The agreement for this case can be expected to be good at high heat fluxes.

Incidentally, a velocity boundary layer thickness should also relate closely to the heat transfer enhancement since the actual velocity of the liquid flowing over the heated surface plays an essential role in the sensible heat transport. According to Rohsenow & Choi (1963), the boundary layer develops up to about 90% of the fully-developed boundary layer at a distance of 0.15 m from the entrance of the channel to the heated surface, on the assumption that the flow is laminar and its velocity is 0.5 m/s. A consideration of the flow effect in the analysis of sensible heat transport would make the present analysis complete.

4.2. Time-averaged heat transfer coefficient

Figure 10 shows the experimental $\bar{h}\sqrt{aT_0}/\lambda$ ($l_b = 0.02$ and 0.01 m) (Monde & Kusuda 1988) plotted against $S_0/\sqrt{aT_0}$, calculated using $S_0 = 71.7\ \mu$m. The solid lines are the same as those in figure 6, and are shown here to compare the theoretical and experimental results. The dashed line is the relation

$$\frac{\bar{h}\sqrt{aT_0}}{\lambda} = 1.65 \times \left(\frac{S_0}{\sqrt{aT_0}}\right)^{-1}, \qquad \delta = \frac{S_0}{\sqrt{aT_0}} > 0.92 \qquad [28]$$

when the thickness of the liquid film $S_0 = 71.7\ \mu$m is utilized,

$$\frac{\bar{h}\sqrt{aT_0}}{\lambda} = 2.3 \times 10^4 \sqrt{aT_0}, \qquad aT_0 < 6 \times 10^{-9}\ \text{m}^2. \qquad [29]$$

Equation [29] was experimentally determined by Monde *et al.* (1988) for the range $aT_0 < 6 \times 10^{-9}$ m^2. It should be noted that the situation indicated by [28] corresponds to the limiting state for $\alpha = 1$. From figure 10, the data of $\bar{h}$ become higher than the values predicted for $\alpha = 1$; this fact is attributed to the influence of the flow. It is interesting to note that most heat transfer data beyond $\alpha = 1$ fall on the dashed line given by [28].

It seems to be rather difficult to understand from figure 10 the effect of the bubble period on the heat transfer enhancement, since the residence time, α, is a function of T_0, as is given by [25]. Figure 11, therefore shows the typical data, $\bar{h}$, plotted against the period, T_0. The solid lines are the theoretical results for $l_b = 0.01$ m at heat fluxes of $q_w = 1.3 \times 10^4$ and 9.0×10^4 W/m^2,

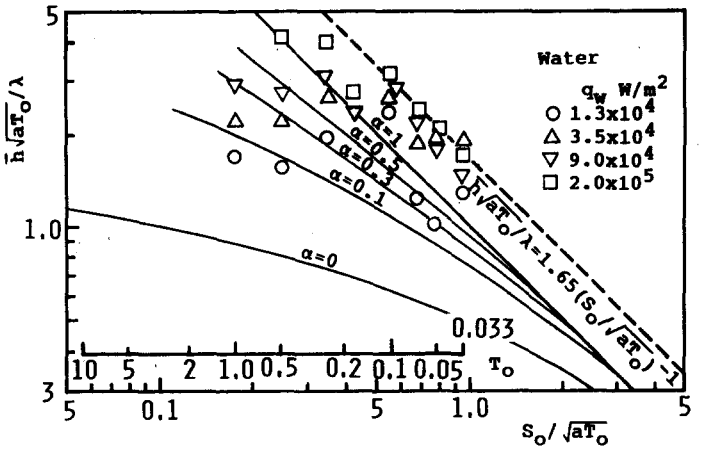

Figure 10. Dimensionless heat transfer, $\bar{h}\sqrt{aT_0}/\lambda$, as a function of dimensionless thickness, $\delta = S_0/\sqrt{aT_0}$, for the experimental data.

respectively. The fact that both the predicted values are nearly equal in spite of the different heat fluxes, is due to neglecting the flow. The two dashed lines are the theoretical results for $S_0 = 50\,\mu$m, $l_b = 0.01$ m and for $S_0 = 100\,\mu$m, $l_b = 0.01$ M at a heat flux of $q_w = 1.3 \times 10^4$ W/m^2, shown for reference. The thin solid line is the theoretical result for $\alpha = 0$. Besides, it may be of interest to compare the heat transfer coefficient obtained with those calculated for a laminar flow in a channel on the assumption that the liquid flows at the same velocity as the rising bubble does. Equation [30] is the solution, derived using an approximate integral method, for forced convection laminar flow on a flat plate with a constant heat flux:

$$\frac{hx}{\lambda} = \frac{0.418}{\left(1-\frac{x_0}{x}\right)^{1/3}}\left(\frac{v}{a}\right)^{1/3}\sqrt{\frac{ux}{v}}, \qquad [30]$$

where the velocity boundary layer begins growing at $x = 0$ and the distance x_0 is the unheated length. The ———— line calculated from [30], gives the local heat transfer coefficients for the rising velocity of the bubble length, $l_b = 0.01$ m, corresponding to the period at the center of the heated surface with the unheated length, $x_0 = 0.15$ m, at which the heated surface is mounted in the experiment (Monde & Kusuda 1988). The ——— line, for reference, is twice as large as the predicted value.

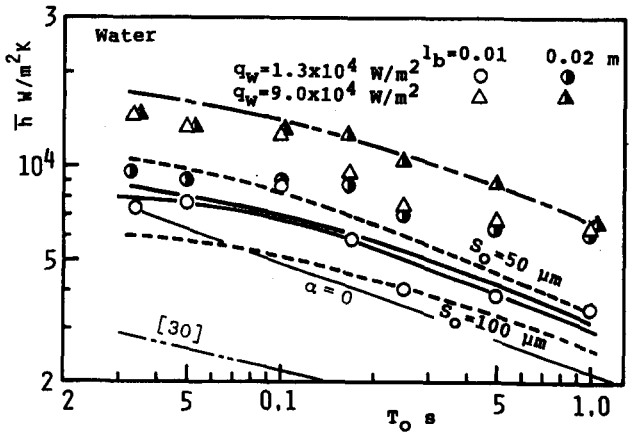

Figure 11. Comparison of the heat transfer coefficients (predicted and measured).

It is found from figure 11 that the experimental data at low heat fluxes are predicted well, while the data at high heat fluxes are about twice as large as the predicted value. This reason is also due to the fact that the flow along the heated surface plays an important role in the heat transfer. Although the agreement becomes less satisfactory for high heat fluxes, the improvement for high heat flux would be expected by taking account of the flow effect, i.e. the convective term, $v(\partial T/\partial y)$, which is related closely to both the thermal and the velocity boundary layers. It may be necessary to say that a similar tendency is obtained for $l_b = 0.03$ m.

Figure 11 shows that the difference between the value of $\bar{h}$ for $q = 9 \times 10^4$ W/m^2 and the predicted values decreases with a decrease in the period. This fact is due to the decrease in the thermal boundary layer thickness, the growth of which is proportional to $\sqrt{aT_0}$, i.e. the thermal boundary layer is hard to be subject to the flow effects.

It should be noted finally that the heat transfer coefficients obtained are more than three times higher than those predicted by [30] and the heat transfer enhancement due to the bubble passage may be promising.

5. CONCLUSIONS

1. A theoretical study has been made of heat transfer enhancement due to bubbles passing through a narrow vertical channel. The results have been compared with existing experimental data.
2. The heat transfer enhancement due to the bubble passage is predicted well in the low heat flux region; agreement becomes less satisfactory for high heat fluxes due to the sensible heat transport added by the flow.

Acknowledgement—Financial support provided by the Japanese Ministry of Education, Science and Culture (Grant No. 62550160) is gratefully acknowledged.

REFERENCES

ISHIBASHI, E. & NISHIKAWA, K. 1960 Saturated boiling heat transfer in a narrow space. *Int. J. Heat Mass Transfer* **12,** 863–894.

KUSUDA, H., MONDE, M., UEHARA, H. & OTSUBO, K. 1981 Bubble influence on boiling heat transfer in a narrow space. *Heat Transfer Jap. Res.* **9,** 49–60.

MONDE, M. 1988 Characteristics of heat transfer enhancement due to bubbles passing through a narrow vertical channel. *J. Heat Transfer* **110,** 1016–1019.

MONDE, M. 1989 Measurement of liquid film thickness during pass of bubbles in a vertical rectangular channel. *J. Heat Transfer*. In press.

MONDE, M. & KUSUDA, H. 1988 Enhancement of heat transfer due to bubbles passing through a narrow vertical rectangular channel. In *Proc. Ist Wld Conf. on Experimental Heat Transfer, Fluid Mechanics and Thermodynamics*, pp. 1459–1465.

MONDE, M., KUSUDA, H., UEHARA, H. & NAKAOKA, T. 1986 Boiling heat transfer in a narrow rectangular channel. In *Proc. 8th Int. Heat Transfer Conf.*, Vol. 4, pp. 2105–2110.

MONDE, M., MIHARA, S. & ONO, Y. 1988 Upper limit of enhancement of boiling heat transfer in a narrow vertical rectangular channel due to passing bubbles. *Wärme-u. Stoffübertrag.* **22,** 91–95.

MONDE, M., MIHARA, S. & NOMA, T. 1989 Enhancement of heat transfers due to bubbles passing through a narrow vertical rectangular channel (effect of subcooling on heat transfer). *Trans. JSME Ser. B* **55,** 483–489 (in Japanese).

NAKASHIMA, K. 1978 Boiling heat transfer outside a horizontal multitube bundle. *Trans. JSME* **42,** 1047–1057 (in Japanese).

ROHSENOW, W. M. & CHOI, H. 1963 *Heat, Mass and Momentum Transfer*, pp. 45–46. Prentice-Hall, Englewood Cliffs, N.J.